Integrative and Comparative Biology

Integrative and Comparative Biology, volume 56, number 5, pp. 973–988
doi:10.1093/icb/icw113

Society for Integrative and Comparative Biology

SYMPOSIUM

Evidence for an Alternative Mechanism of Toxin Production in the Box Jellyfish *Alatina alata*

Cheryl Lewis Ames[1,*,†] and Jason Macrander[‡]

[*]Department of Invertebrate Zoology, National Museum of Natural History, Smithsonian Institution, Washington, DC 20013, USA; [†]Biological Sciences Graduate Program, University of Maryland, College Park, MD 20742, USA; [‡]Department of Evolution, Ecology, and Organismal Biology, The Ohio State University, Columbus, OH 43215, USA

From the symposium "Integrative and Comparative Biology of Venom" presented at the annual meeting of the Society for Integrative and Comparative Biology, January 3–7, 2016 at Portland, Oregon.

[1]E-mail: amesc@si.edu

Synopsis Cubozoans (box jellyfish) have a reputation as the most venomous animals on the planet. Herein, we provide a review of cubozoan prey capture and digestion informed by the scientific literature. Like all cnidarians, box jellyfish envenomation originates from structures secreted within nematocyte post-Golgi vesicles called nematocysts. When tentacles come in contact with prey or would-be predators, a cocktail of toxins is rapidly deployed from nematocysts via a long spiny tubule that serves to immobilize the target organism. The implication has long been that toxin peptides and proteins making up the venom within the nematocyst capsule are secreted directly by nematocytes during nematogenesis. However, our combined molecular and morphological analysis of the venomous box jellyfish *Alatina alata* suggests that gland cells with possible dual roles in secreting toxins and toxic-like enzymes are found in the gastric cirri. These putative gland cell assemblages might be functionally important internally (digestion of prey) as well as externally (envenomation) in cubozoans. Despite the absence of nematocysts in the gastric cirri of mature *A. alata* medusae, this area of the digestive system appears to be the region of the body where venom-implicated gene products are found in highest abundance, challenging the idea that in cnidarians venom is synthesized exclusively in, or nearby, nematocysts. In an effort to uncover evidence for a central area enriched in gland cells associated with the gastric cirri we provide a comparative description of the morphology of the digestive structures of *A. alata* and *Carybdea* box jellyfish species. Finally, we conduct a multi-faceted analysis of the gene ontology terms associated with venom-implicated genes expressed in the tentacle/pedalium and gastric cirri, with a particular emphasis on zinc metalloprotease homologs and genes encoding other bioactive proteins that are abundant in the *A. alata* transcriptome.

Introduction

Box jellyfish (Cnidaria: Cubozoa) are the most venomous animals in the world (Barnes 1966; Bentlage et al. 2010; Gershwin et al. 2010). Box jellyfish envenomation originates from intracellular structures called nematocysts (Fig. 1a), which are produced by specialized cells called nematocytes through a secretory pathway (Slautterback and Fawcett 1959; Ozbek 2011). These microscopic venom-filled capsules are highly concentrated in the tentacles and are vital for prey capture and defense (Hessinger and Lenhoff 1988; Gershwin 2006). Tissue-specific transcriptome analyses of the venomous box jellyfish *Alatina alata* revealed that candidate venom and nematocyst development (nematogenesis) genes were abundant in the tentacle at the base of the adjoining pedalium, while additional venom-implicated genes were also highly expressed in the gastric cirri (Lewis et al. 2016). Box jellyfish digestion is presumed to be facilitated by gastric cirri, which in most cubozoans are coalesced into four distinct structures called the gastric phacellae, within the quadrangular stomach (Larson 1976; Conant 1897; Conant 1898; Bentlage and Lewis 2012). Nematocysts in the gastric cirri are thought to aid in incapacitation and digestion of prey items (Larson 1976; Jouiaei et al. 2015b). However, mature medusae of the emerging cubozoan model *Alatina alata* lack nematocysts in the gastric cirri (Gershwin 2005; Lewis et al. 2013; Lewis Ames et al. 2016) suggesting that an alternative secretory mechanism may

be responsible for venom produced for prey incapacitation, and possibly digestion, in this species. In Cnidaria it has been proposed that nematocysts synthesize and store toxic peptides for envenomation (Beckmann and Özbek 2012). However, nematogenesis is not the only pathway in which venom is produced (Moran et al. 2012, 2013). Additional examination of the ultrastructure of the gastric cirri and digestion activity in cubozoans will aid in elucidating the presence of gland cells with a possible role in the secretion of venom-associated gene products.

Venom serves as both a foraging and defensive adaptation, with the majority of venomous animals relying on bioactive venom components during trophic interactions (Casewell et al. 2012). It has been suggested that among a variety of venomous lineages, toxic components making up the venom have evolved as a by-product of securing and digesting prey (Mackessy et al. 2003) (for a review see Bottrall et al. 2010; Casewell et al. 2012; Junqueira-de-Azevedo et al. 2015). Many enzyme protein families have been recruited to aid in prey capture and digestion in metazoans, ultimately as secretions of the venom gland during envenomation (Mali et al. 2004; Nevalainen et al. 2004; Calvete et al. 2009; Fry et al. 2009; Bottrall et al. 2010; Casewell et al. 2012; Junqueira-de-Azevedo et al. 2015). Due to the potential dual role of these proteins as digestive enzymes and toxic-like components of venom, demarcation between envenomation and digestion is often attributed to alternative origins of venom production linked to a single point of envenomation (Bottrall et al. 2010; Junqueira-de-Azevedo et al. 2015). In cnidarians, discernment between bioactive proteins that function in envenomation (subduing prey or in defense) and those used in prey digestion is even more complicated, as no centralized gland-like structure appears to be responsible for producing toxins and/or toxic-like enzymes (Fautin and Mariscal 1991; Basulto et al. 2006; Moran et al. 2013; Lewis Ames et al. 2016z; Macrander et al. 2016).

More stringent morphological and molecular analyses are needed to test hypotheses regarding the dual role certain toxic-like enzymes might have internally (digestion of prey) as well as externally (envenomation). To better understand venom diversity and mechanisms controlling venom synthesis in *A. alata*, we describe the morphology of the gastric cirri and other structures within the digestive system, review prey capture and digestion in cubozoans, analyze the publically available *A. alata* transcriptome for potentially overlooked venom-like transcripts, and conduct a comparative analysis of the gene ontology (GO) of differentially expressed toxin gene candidates within the gastric cirri and tentacle/pedalium that were not evaluated previously.

Methods

Morphological data

Collectively the gross morphology, sting potency, life history, sexual behavior, and worldwide distribution of *A. alata* are well-documented (Arneson and Cutress 1976; Chung et al. 2001; Chiaverano et al. 2013; Lewis et al. 2013; Carrette et al. 2014; Lawley et al. 2016; Lewis et al. 2016). Lewis Ames et al. 2016 In this study, *A. alata* medusae were collected in Bonaire, The Netherlands during monthly spawning aggregations (8–10 days after the full moon) in 2011, 2015, and 2016. No prey items were observed within the stomach or adhered to the tentacle at any time. Photographs and video were taken using light microscopy of gastric phacellae (composed of numerous cirri) excised from a live *A. alata* medusa (bell height ~70 mm) (Fig. 2; Supplementary File S1). Additionally, the gastric phacella was excised from a preserved (8% formalin) *A. alata* museum voucher in the Smithsonian National Museum of Natural History (USNM1195804), and homogenized tissue was examined using light microscopy (600× and 1000× magnification) and photographed (Fig. 2c,e).

Molecular data

Sequencing, library preparation, and *A. alata* transcriptome assembly were reported previously (Lewis Ames et al. 2016). Briefly, total RNA sequenced from multiple body parts (including the gastric cirri and tentacle/pedalium) was prepared using the paired-end, 100 bp sequencing kit for the Illumina HiSeq 2500, trimmed using TrimGlaore! (Krueger 2012), filtered using Allpaths Error Correction (Gnerre et al. 2011), and assembled *de novo* using Trinity (Grabherr et al. 2011; Haas et al. 2013). The resulting ~126K Trinity transcripts (CEGMA completeness score = 99%) were further reduced to a subset of ~32K transcripts at a 1.5 FPKM (fragments per kilo base per million fragments mapped) threshold. The *A. alata* transcriptome Shotgun Assembly project is available at DDBJ/ENA/GenBank under the accession GEUJ01000000.

Evaluation of previous *de novo* transcriptome assembly

Candidate toxin genes were screened to determine if multi-copy isoforms from candidate toxins were incorrectly assembled into a single transcript (as per Macrander et al. 2015) during *de novo* assembly of the *A. alata* transcriptome (Lewis Ames et al. 2016).

The original paired-end raw reads (BioSampleSAM4569893 and BioSampleSAM4569895, corresponding to BioProject PRJNA312373) were mapped to candidate toxin transcripts in bowtie (v. 1.0.0) with default settings, except for trimming the first five bases from the raw reads (Langmead et al. 2009). The candidate toxin transcripts and mapped reads were then imported into Geneious version 7.1.9 (Kearse et al. 2012) and visually inspected for polymorphisms that may be indicative of misincorporated isoforms. If only a single polymorphism was recovered consistently among the mapped reads, it was treated as a potential heterozygote. If more than one polymorphism was recovered, a *de novo* assembly for those transcripts was done using the Geneious assembler with the following constraints: gaps per read of 20%, max gap size of 5, min overlap of 75, word length of 12, reanalyze threshold of 4, and maximum ambiguity of 16. The *de novo* assembled contigs were then reexamined for polymorphisms in the assembly.

RSEM and differential expression (EdgeR)

Relative gene expression was calculated for the gastric cirri and tentacle/pedalium using the program RSEM (Li and Dewey 2011). Raw reads from the gastric cirri and tentacle/pedalium were mapped to the *A. alata* transcriptome (Lewis Ames et al. 2016). Differences in gene expression were calculated between the gastric cirri and tentacle/pedalium samples in the EdgeR Bioconductor package (Robinson et al. 2010). Resulting transcripts were then used as query sequences in a tBLASTn search against the UniProt database. BLAST hits with GO information were used in combination with a custom python script (Supplementary File S2) to average the expression values derived from the matrix produced by EdgeR across all GO groups. This approach accounts for overly abundant GO groups, while still considering differences in gene expression in GO assignment. Upregulated GO groups and calculated GO specific expression values were visualized in the program REVIGO (Supek et al. 2011) for the biological process (BP) and molecular function (MF) GO domains in the gastric cirri and tentacle/pedalium.

Identification of unknown toxins

In addition to characterizing nematogenesis proteins and previously characterized box jellyfish toxins (Supplementary File S3), we identified additional candidate toxic-like transcripts within the transcriptome. Transcripts were translated into protein sequences in the program TransDecoder (http://transdecoder.github.io/), with an open reading frame of 50 or more amino acids. The program SignalP (Petersen et al. 2011) was used to identify transcripts containing a signaling region. Signal peptides have been identified in transcripts encoding peptides secreted within nematocytes as structural elements of nematocysts (i.e., complex secretory organelles) (Anderluh et al. 2000; David et al. 2008; Zenkert et al. 2011). Here, we also sought to identify signal peptides in the gastric cirri which lack nematocysts, given the predicted presence of putative venom gland cells associated with the gastric cirri (Lewis Ames et al. 2016). Toxic-like sequences were identified in tBLASTn using annotated toxin peptides against the ToxProt database (http://www.uniprot.org/program/Toxins). Abundance of zinc metalloproteases, one of the more abundant toxin gene candidates, was further evaluated to determine where candidate toxins were most abundant in the *A. alata* transcriptome. Amino acid sequences were aligned in MAFFT (Katoh and Standley 2013) using the L-INS-i algorithm, BLOSUM62 scoring matrix, 1.53 gap open penalty, and 0.123 offset value, alongside zinc metalloproteases from several venomous and non-venomous animal species (obtained from NCBI GenBank). A zinc metalloprotease gene tree was constructed in the program FastTree (Price et al. 2010) with default settings and 1000 bootstrap replicates using seqboot in the PHYLIP package (Felsenstein 2009) (Supplementary Fig. S1).

Results and discussion

Prey capture and incapacitation in cubozoans

From the limited accounts of cubozoan prey capture that have been documented in natural settings, it is evident that box jellyfish feed on a variety of prey items (Table 1). An ontogenetic shift in diet has been correlated with modifications in nematocyst composition in some cubozoans (Carrette et al. 2002; Júnior and Haddad 2008), suggesting that certain nematocyst types are more suitable for taxon- or size-specific prey capture (McClounan and Seymour 2012; Acevedo et al. 2013). Free amino acids released by potential prey items may illicit a response by the tentacles (Larson 1976), resulting in prey capture and immobilization due to injection of bioactive proteins by nematocysts (David and Challoner 1974; David et al. 2008; Özbek et al. 2009; Beckmann and Özbek 2012). The captured prey is brought to the mouth lips of the manubrium (feeding tube) by the contracting tentacles and bending pedalium, and is transported via ciliary action and muscle contraction (Larson 1976; Hamner et al. 1995; Stewart 1996) into the transparent stomach cavity located at the apex of the box jellyfish (Figs. 1b,c and 3).

Table 1 Review of cubozoan species prey items and geographical location

Cubozoan family	Cubozoan species	Prey item(s)	Geographical location	Reference(s)
Alatinidae	*Alatina alata*	Plankton (?), larval fish, caridean shrimps, polychaetes	Puerto Rico, USA (Atlantic Ocean)	Arneson and Cutress (1976); R. N. Larson, Personal communication (Fig. 2a); Lewis et al. 2013
Carukiidae	*Malo filipina*	Rabbitfish	Aurora, The Philippines (Pacific Ocean)	S. Tuason, Personal communication (Fig. 2b)
Carukiidae	*Carukia barnesi*	Plankton, larval fish (*Acanthochromis* sp.)	Double Island, North Queensland, Australia (Pacific Ocean)	Courtney et al. 2015
Tamoyidae	*Tamoya haplonema*	fish (*Teleostei*)	Shangrilá and Paraná, Brazil (Atlantic Ocean)	Júnior and Haddad 2008
Carybdeidae	*Carybdea xaymacana* (as *C. marsupialis*)	Polychaetes (*Ceratonereis*), crustaceans (*Acartia*), fish (*Jenkinsia*), and eel larvae	Puerto Rico, USA (Atlantic Ocean)	Larson 1976; R. N. Larson, Personal communication(Fig. 2c)
Carybdeidae	*Carybdea marsupialis*	Plankton	Alicante, Spain (Adriatic Sea)	Acevedo et al. 2013
Carybdeidae	*Carybdea brevipedalia* (as *C. rastonii*)	Fish	Shizuoka, Japan (Pacific Ocean)	Ishida 1936
Carybdeidae	*Carybdea rastonii*	Msids, larval fish	Hawaii, USA (Pacific Ocean)	Matsumoto 1995
Tripedaliidae	*Tripedalia cystophora*	Copepods (*Oithano nana*)	Puerto Rico, USA (Atlantic Ocean)	Stewart 1996
Tripedaliidae	*Copula sivickisi*	Polychaetes heteronereids, gammarid amphipods, cumaceans	Magnetic Island, Townsville, Australia (Pacific Ocean)	Hartwick 1991
Chiropsalmidae	*Chiropsalmus quadrumanus*	Crustaceans: sergetid shrimp (*Peisos petrunkevitchi*), peneoidean and caridean shrimps, *Lucifer*, brachyura larvae, isopods, crabs; nematodes, fish, fish eggs	Shangrilá and Paraná, Brazil (Atlantic Ocean)	Larson 1976; Júnior and Haddad 2008
Chiropsalmidae	*Chiropsalmus* sp.	Shrimp (*Actes australia*)	Australia (Pacific Ocean)	Carrette et al. 2002; Barnes 1966
Chirodropidae	*Chironex fleckeri*	Shrimp (*Actes australia*), fish	Australia (Pacific Ocean)	Barnes 1966; Hamner et al. 1995; Carrette et al. 2002

Depending on the cubozoan species, prey items coming in contact with tentacles are either immobilized upon contact, but remain writhing until they are inserted into the manubrium, or paralyzed almost immediately. Figure 1b–d compares prey capture by three species of box jellyfish varying in size from ~100 mm (*A. alata*) to ~40 mm (*Carybdea xaymacana* and *Malo filipina*), with the two smaller species catching and ingesting prey items larger than their own bell size. Although there is no accepted explanation for the discrepancy seen in cubozoan prey types, we suspect that both nematocyst type and venom potency are important factors related to prey size. Cubozoan tentacles are composed of both circular and longitudinal muscle fibers made up of rings of nematocysts arranged around a longitudinal canal that runs the length of the tentacle lumen (Southcott 1967). Some box jellyfish species also have nematocysts along the mouth lips and within the gastric cirri (Gershwin 2006), which are thought to aid in securing large prey within the manubrium (Larson 1976) (Fig. 1c). Additionally, the holding capacity (volume) of the transparent stomach cavity varies among cubozoan species (Bentlage and Lewis 2012), with some species having a deep, broad stomach (Collins et al. 2011), while other cubozoans, like *A. alata*, have a shallow stomach and a short wide manubrium that expands to match the width of the stomach (Lewis et al. 2013) (Fig. 2b). We hypothesize that since cubozoans with potent stings (e.g., *M. filipina* and *A. alata*) (Chung et al. 2001; Bentlage and Lewis 2012) could potentially incapacitate and kill prey prior to ingestion, they do not require nematocysts in the digestive system. Conversely, box jellyfish with comparatively milder stings (e.g., *Carybdea* species) (Di Camillo et al. 2006) can ingest prey items that are disproportionately large in comparison to the size of the stomach,

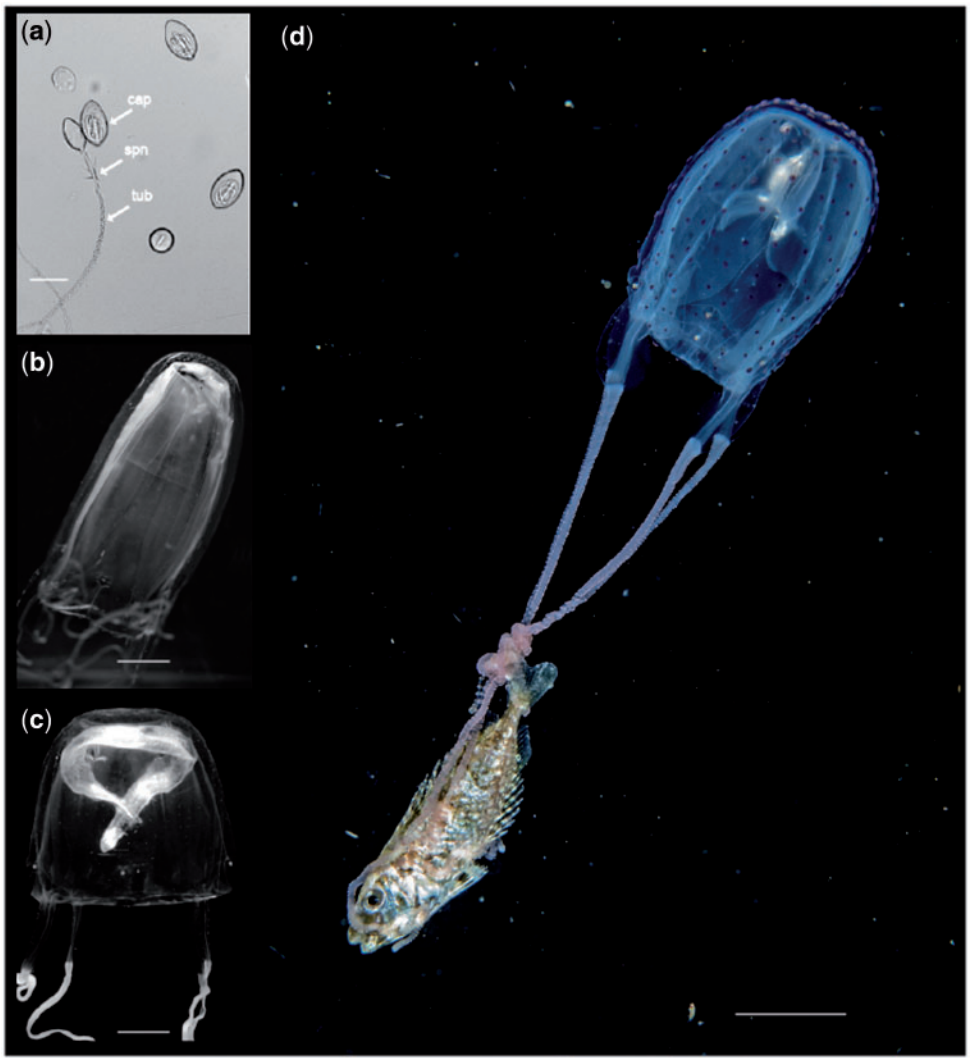

Fig. 1 (**a**–**d**) Feeding in cubozoans. (a) Penetrant nematocysts (euryteles) isolated from the tentacles of *Alatina alata* in this study (Bonaire, the Netherlands). Four intact nematocysts seen on the right and a single discharged nematocyst seen on the left revealing the long spiny penetrant tubule. (b) *Alatina alata* feeding on a larval fish corresponding to the small thin dark black object lying horizontal in the stomach (Puerto Rico). Photo courtesy of Ron N. Larson. (c) *Carybdea xayacana* feeding on a larval eel almost twice the bell width, folded up inside the stomach with head and tail pushed down within the central feeding tube (manubrium) (Puerto Rico). Photo courtesy of Ron N. Larson. (d) *Malo filipina* seconds after having captured and killed a young Rabbitfish (Aurora, The Philippines). Photo courtesy of Scott Tuason. Abbreviations cap = capsule; spn = spines; tub = tubule. Scale bar a = 30 μm, b–d = 10 mm.

possibly due to the presence of nematocysts in the gastric cirri that further incapacitate prey (Conant 1898; Larson 1976). Ultimately, it is most likely the cocktail of bioactive proteins secreted from the gastric cirri that is responsible for killing and digesting prey (Conant 1898; Ishida 1936; Larson 1976).

Anatomy of the stomach and gastrovascular system in *Carybdea* and *Alatina alata*

Herein we show that the internal anatomy of the digestive structures (i.e., the digestive system) of *A. alata* shares some morphological characters with the digestive system of *Carybdea xaymacana* on which a histological study was conducted more than 115 years ago (Conant 1898).

Gastric cirri morphology

At each corner of the stomach these cubozoans possess four interradial gastric phacellae composed of multiple tufts of gastric cirri attached to one (*Carybdea*) or multiple (*A. alata*) stalks that are outgrowths of the lower stomach wall (Figs. 2 and 3). In both *C. xaymacana* and *A. alata*, and possibly all cubozoans with gastric cirri, the highly contractile gastric cirri are covered in thick mucus, whose provenance has been attributed to the mucus-containing goblet cells of the stomach (Conant 1898). One

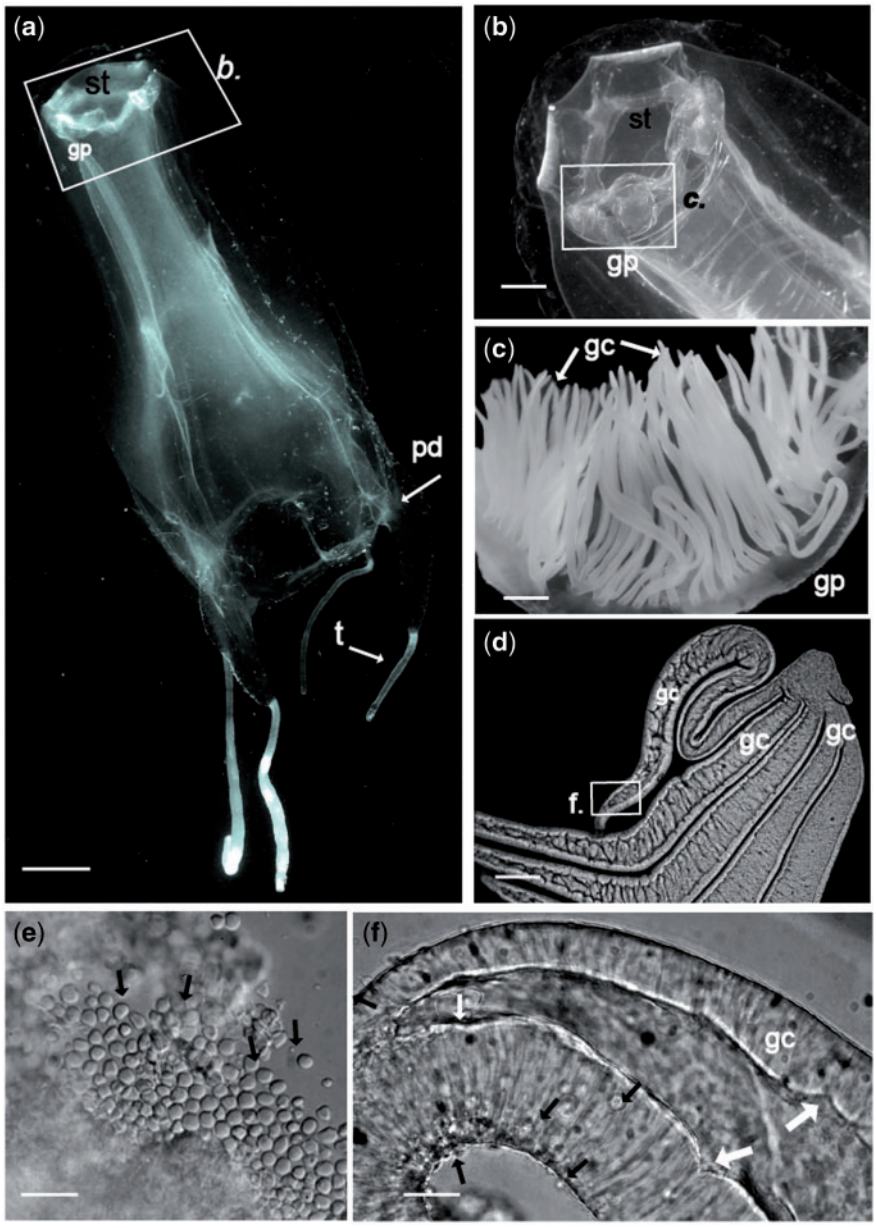

Fig 2 (**a**–**e**) *Alatina alata* box jellyfish from Kralendijk, Bonaire, The Netherlands (October 29, 2016; 12:00). (a) Live mature *A. alata* box jellyfish swimming in the water nearshore, during a monthly spermcasting aggregation. The white box identifies the area on the transparent apex where the four gastric phacellae can be seen in each corner of the stomach. (b) A magnification of the area highlighted in 1a of the *A. alata* apex. The white box highlights one of the four gastric phacellae found at each corner of the stomach. (c) A single gastric phacella removed from the corner of the stomach of a preserved *A. alata* specimen (USNM 1195804). (d) A tuft from a single gastric phacella removed from the corner of the stomach of a live *A. alata* box jellyfish. A membrane outlines each of the five individual gastric cirri forming the tuft. The appearance of horizontal ridges within the lumen corresponds to the somewhat regular pattern of constrictions along the length that connect with channels extending through the outer membrane to the stomach. (e) Black arrows point to the remains of a macerated gastric phacella composed almost entirely of granules excised from the stomach of a preserved (8% formalin) *A. alata* medusa. (f) A magnification of the area highlighted in 1d of a single gastric cirrus. White arrows indicate areas where the lumen pinches into the membrane of the gastric cirrus. Black arrows indicate tiny non-nucleated granules circulating within the lumen that are transported across the outer membrane via channels (putative duct) into the stomach. Abbreviations gc = gastric cirrus, gp = gastric phacella, pd = pedalium, st = stomach, t = tentacle. Scale bars: a, 10 mm; b. 3 mm; c. 1 mm; d 0.5 mm; e. 130 μm; f. 0.10 mm.

major difference between the internal anatomy of *C. xaymacana* and *A. alata* is the lack of nematocysts in the digestive system of mature *A. alata* medusae (Gershwin 2005; Lewis et al. 2013; Lewis Ames et al. 2016). In this study, we found that a single tuft of five gastric cirri that was dissected from the stomach of a live *A. alata* medusa (Fig. 2b,d,f) writhed and constricted continuously on a microscope slide in

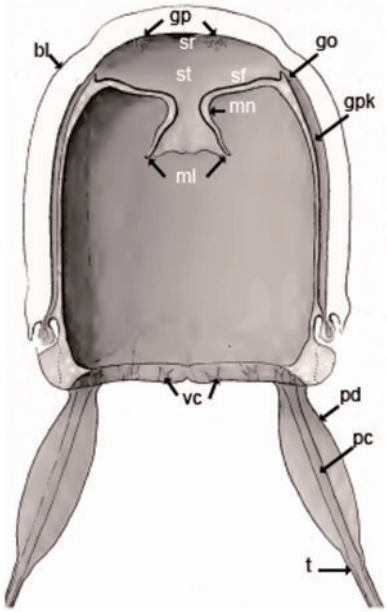

Fig. 3 Schematic of the internal anatomy of box jellyfish *Carybdea*. A *Carybdea* bell cut in haf longitudinally at the perradius (along the vertical axis at the mid-point between opposing tentacles). Dark shading indicates the gastrovascular system in which the fluids in the stomach are shuttled to the gastric pockets (gastro vascular cavity) via four gastric ostia (only two shown here) located on each side of the bell. A connection between the gastric pockets and the tentacles is facilitated via a circular channel around the perimeter of the base of the bell (not shown here) giving rise to four pedalial canals (only two shown here) and multiple marginal velarial canals (eight per quadrant). Abbreviations b = bell, go = gastric ostium, gp = gastric phacellae, gpk = gastric pocket, ml = mouth lips, mn = manubrium (feeding tube), pc = pedalial canal, pd = pedalium, sf = stomach floor, sr = stomach roof, st = stomach, t = tentacle, vc = velarial canals. *Carybdea xaymacana* box jellyfish depicted here ~30 mm in bell height. Modified from (Conant 1898).

what appeared to be a thin layer of mucus (Supplementary File S1). Careful examination of the gastric cirri tuft using light microscopy revealed a membrane outlining the periphery of each gastric cirrus, uniting them at the base (the stalk), and creating a shared space among the gastric cirri (Fig. 2d). Within the shared space, numerous non-nucleated membrane bound granules (10–15 μm in diameter) were seen being transported from the stalk toward the distal tips of the gastric cirri (Fig. 2f; Supplementary File S1). Horizontal striations were observed in a somewhat regular pattern within the lumens of the cirri, which are filled with supportive gelatin. Magnification revealed that the apparent striations corresponded to numerous internal invaginations in the wall of the lumen giving rise to duct-like channels that pass through the external membrane (Fig. 2d,f). Granules were witnessed being transported through the duct-like channels across the membrane, and secreted into what would be the stomach *in vivo* (Supplementary File S1). The contents of the granules were not examined in this study. However, macerated gastric cirri tissue dissected from a preserved *A. alata* museum specimen was found to be composed almost entirely of granules (Fig. 2e) similar in size and morphology to those secreted by the gastric cirri of a live *A. alata* box jellyfish (Fig. 2f). These granules also match the description of granules associated with glandular cells of *C. xaymacana* (Conant 1898) and *Nematostella vectensis* (Moran et al. 2013).

Prey digestion

Within the stomach of *C. xaymacana*, prey are held in place by the gastric cirri, where nematocysts likely aid in prey stabilization and incapacitation (Larson 1976). Prey items within the stomach are covered by mucus secreted by the gastric phacellae and stomach wall that exhibits extracellular protease activity (Larson 1976). Functional assays utilizing mucus recovered from the manubrium, gastric fluid (from the stomach cavity), and phacellae of *C. brevipedalia* (as *C. rastonii*) revealed that even in the absence of prey items, tryptase activity was elevated in gastric phacellae, but not in the rest of the digestive system (Ishida 1936). However, after prey items were introduced, tryptase activity became elevated in the gastric fluid, and within hours was equal to levels initially measured in the gastric phacellae (Ishida 1936). Tryptase detected in the gastric fluid and manubrium was presumed to be secreted from the gastric phacellae under normal circumstances, but in response to prey ingestion it filled the entire digestive system to facilitate extracellular digestion (Ishida 1936). Digestion in *Carybdea* species, and cubozoans in general, has been described as a relatively rapid process, taking only a few hours (Ishida 1936; Larson 1976; Hamner et al. 1995; Acevedo et al. 2013). During digestion, food particles are seen circulating directionally through the transparent gastrovascular system of the box jellyfish (Larson 1976; Hamner et al. 1995). Conant (1898) noted that "the digestive juices left the nervous system of the fish intact so that from the stomach of *C. xaymacana* could be obtained beautiful dissections, or rather macerations, of the brain, cord, and lateral nerves of a small fish." Digestion is considered finished when debris (e.g., fish scales and eyes) is regurgitated from the manubrium, and new prey items are ingested (Barnes 1966; Larson 1976).

Circulation of gastric fluids and nutrients

In *Carybdea* and *A. alata* the four gastric ostia open perradially at a point between adjacent gastric

phacellae, on each of the four walls of the stomach (Figs. 2a,b and 3). Each ostium is contiguous with one of the four gastric pockets occupying each side of the bell (Fig. 3), which are separated from one another by thin strips of interradial vascular lamella. Gastric ostia serve as channels connecting the stomach to the peripheral portion of the gastrovascular system which branches into velarial canals at the base of the bell, called the velarial turnover. Movement of fluids (e.g., nutrients) into the gastrovascular system and expulsion of waste or reproductive material are regulated by the flexible lower margin of each gastric ostium that forms a valve (Fig. 3). A circular canal runs the perimeter of the bell, near the velarial turnover, and gives rise to one pedalial canal at each of the four corners of the bell that passes through the center of each pedalium (the wide, wing-like structure at the base of each tentacle) and into the tentacle lumen (Fig. 3). Tentacles are hollow, tube-like structures consisting of a series of stacked rings of nematocysts connected by collagen fibers. Nematocysts in the tentacles are in direct communication with the gastrovascular system by way of fluids circulating in and out of the pedalial canal and tentacle lumen.

Venom and digestive secretory products

In many venomous animals, paralogous proteins with respective roles in venom and digestion are synthesized in separate organs (Junqueira-de-Azevedo et al. 2015). However, in box jellyfish, neither a venom gland nor a digestive gland has been documented. Recently, the presence of putative gland cells in the gastric cirri of *A. alata* has been proposed (Lewis Ames et al. 2016). This, together with the morphological evidence presented herein, supports the notion that granules secreted by the gastric cirri may be pre-packaged toxins and toxin-like enzymes representing an alternative mode of toxin production for prey incapacitation within the stomach. Furthermore, these putative "toxin granules" might also be transported to nematogenic regions in the tentacle at the base of the pedalium (Lewis Ames et al. 2016) for recruitment into developing nematocysts. The secretory nature of the granules in the digestive system of *A. alata* (this study) and *C. xaymacana* (Conant 1898; Larson 1976) appears functionally similar to gland cells recently identified in a sea anemone that secrete toxins independent of nematocytes (Moran et al. 2012, 2013). If this putative assemblage of gland cells is in fact a central point of secretion of toxins and toxic-like enzymes with roles in envenomation, this would represent the first such gland-like structure in cubozoans. It is possible that the same bioactive proteins used in venom are also used in prey digestion. However, testing this hypothesized dual role of gland cells awaits functional studies conducted during prey capture and digestion, and gene localization studies within the digestive system of *A. alata* and other cubozoans.

Evaluation of *de novo* assembly

In total we evaluated 154 candidate toxin-like transcripts to validate whether the *A. alata* transcriptome assembly (Lewis Ames et al. 2016) might have inadvertently misincorporated certain raw reads as a single transcript that in fact belong to multiple toxin gene copies but with low sequence variation (Macrander et al. 2015). By mapping the raw reads back to the transcripts we determined that the majority of the original transcripts had been properly recovered in the original transcriptome; for 52 transcripts we recovered potential heterozygous alleles. Beyond these, no additional "hidden" toxin gene copies or alleles were recovered from the original *A. alata* transcriptome assembly. Given the stringent parameters employed by the authors during the initial *A. alata* transcriptome assembly, it appears that any problematic transcripts were appropriately removed, resulting in a high quality transcriptome that serves as an excellent tool for additional gene discovery in cubozoans.

Tissue-specific expression of candidate toxins

Within the tentacle/pedalium, the most abundant transcripts identified using BLAST were structural in nature (e.g., collagens), with many involved in nematogenesis (e.g., minicollagens) (Fig. 4). Conversely, transcripts for venom-associated candidate genes were expressed at much higher levels in the gastric cirri, with serine proteases, metalloproteases, and GM2 ganglioside collectively being expressed in higher proportions than any group of venom-associated candidates in the tentacles (Fig. 4). Among the focal gene candidates in this analysis, zinc metalloprotease transcripts were in high abundance in both the tentacle/pedalium and gastric cirri (Fig. 4). Zinc metalloproteases make up a major component of venom in many species by activating toxins or acting as toxins (Calvete et al. 2009), and are reported to exhibit a dual role in initial prey immobilization during envenomation and in prey digestion in some snakes (Bottrall et al. 2010).

In cnidarians, zinc metalloproteases are reportedly deployed from nematocysts in the tentacles (Pan et al. 1998; Chera et al. 2006; Avila 2009; Balasubramanian et al. 2012; Casewell et al. 2012;

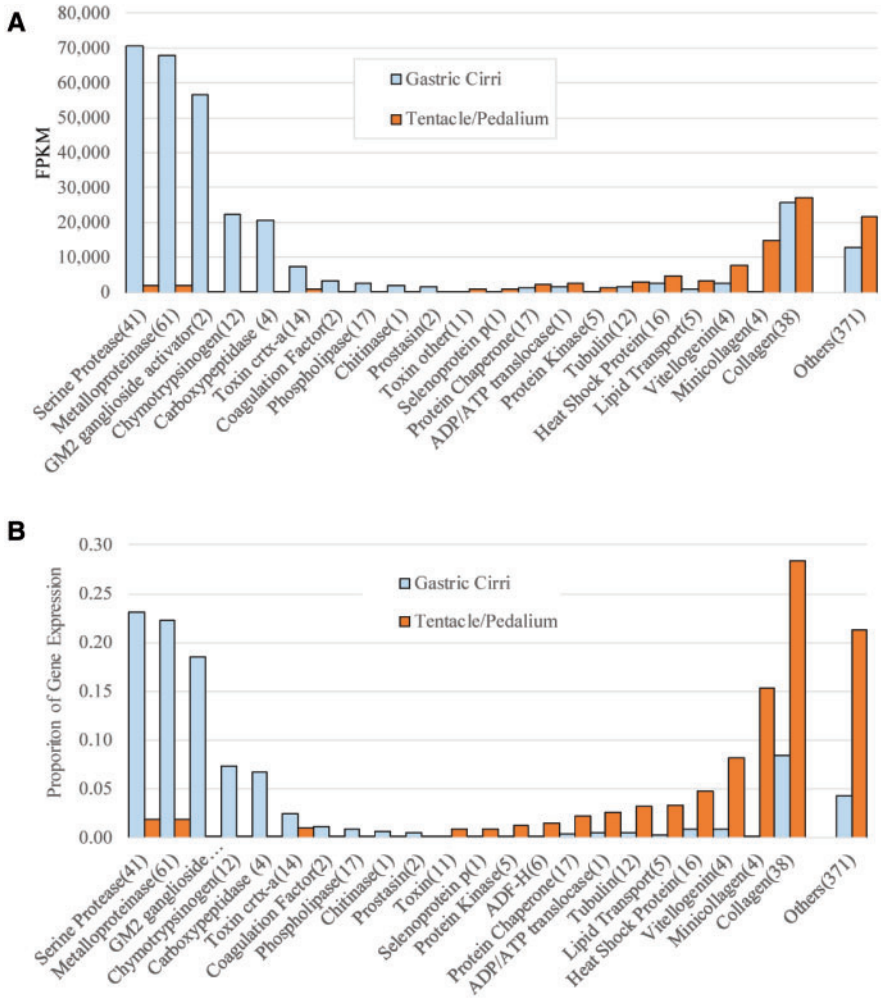

Fig 4 Expression level (FPKM) comparisons of box jellyfish toxins and nematocysts associated proteins in the gastric cirri and tentacle (with adjoining pedalium base). Expression values for each group of genes are represented as either (**a**) FPKM or (**b**) percent of focal candidate gene expression. Numbers in parentheses indicate how many transcripts were identified for each of the toxin or nematocyst associated proteins.

Gacesa et al. 2015; Ponce et al. 2015; Ponce et al. 2016) in combination with other venom components to disable homeostatic processes in the target organism. Recent investigations using a broad phylogenetic approach have identified a non-toxin origin of these toxic-like enzymes, suggesting that they have been incorporated into cnidarian venom multiple times (Moran et al. 2013; Rachamim et al. 2014). To elucidate evolutionary relationships among the toxin-like zinc metalloproteases identified in our study, we constructed a gene tree that includes 44 candidate zinc metalloprotease transcripts from *A. alata*, and previously characterized, publically available metazoan zinc metalloproteases, representing a total of 316 zinc metalloprotease sequences. The *A. alata* candidate zinc metalloprotease transcripts were found throughout the gene tree, with many individual gene clusters having high bootstrap support, but low support between gene clusters (Supplementary Fig. S1). When evaluating individual transcript expression levels in combination with the gene tree analyses, our findings did not reveal any regions of the gene tree corresponding to particular candidate zinc metalloproteases that were consistently expressed at higher levels in either the tentacle or gastric cirri (Supplementary Fig. S1). These results suggest that in a comparative context the zinc metalloproteases identified in our study do not appear to be expressed at higher levels in the tentacles of *A. alata*, which is contrary to the notion that in cnidarians these, and other toxic-like enzymes with venom-related roles, are produced solely in nematocysts (Jouiaei et al. 2015b).

Differential expression and gene ontologies

Our EdgeR analysis identified 1871 transcripts that were differentially expressed between *A. alata* gastric

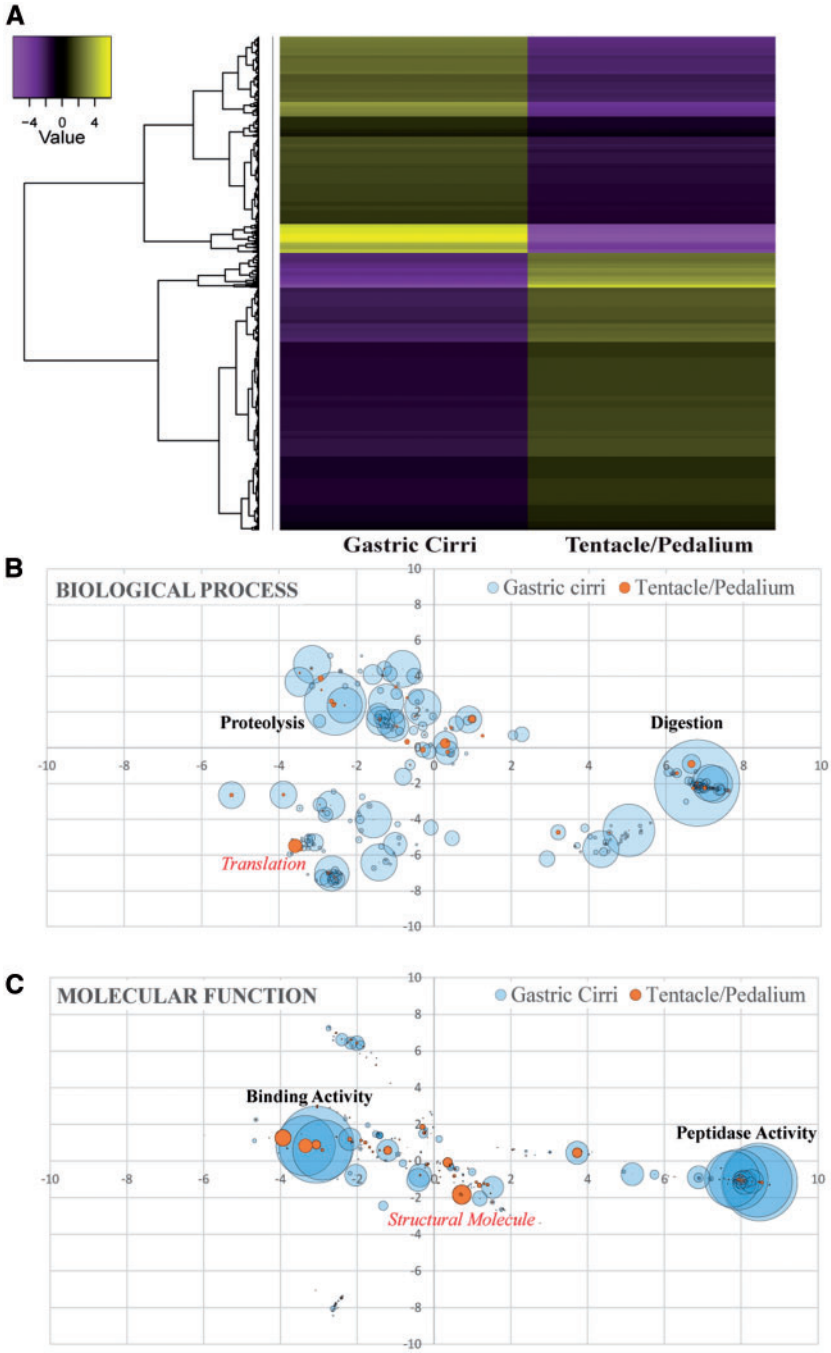

Fig. 5 Differential gene expression and GO summary for *Alatina alata*. (**a**) Heatmap for gastric cirri and tentacle (with adjoining pedalium base), with REVIGO plots depicting overall expression of identified gene ontology (GO) groups in the (**b**) BP and (**c**) MF domains. (b) Within the BP domain, transcripts with GO groups associated with proteolysis and digestion were significantly more abundant in the gastric cirri, while the most notable GO group from the tentacle/pedalium was associated with translation. (c) Within the MF domain, GO groups closely associated with peptidase and binding activity were most abundant in the gastric cirri, while GO groups associated with structural molecules were most abundant in the tentacle/pedalium.

cirri and tentacle/pedalium. Of these transcripts, 1260 had significant BLAST hits against the UniProt database, of which 1223 were functionally categorized in a variety of GO groups. Among these, the most abundant unique GO groups were visualized in the program REVIGO (Fig. 5). Overall we identified a significantly higher ratio of GO groups in the gastric cirri when compared with the tentacle/pedalium (Fig. 5). Within the GO BP domain, transcripts associated with digestion and proteolysis were in highest abundance. In the MF domain, transcripts involved in peptidase and

Table 2 Ten most abundant candidate toxic-like sequences and transcripts with signaling region for gastric cirri (GC FPKM) and tentacle/pedalium (TP FPKM).

ToxProt Top BLAST hits					
Transcript	**GC FKPM**	***E*-value**	**ID**	**Protein names**	**Organism**
comp63246_c0_seq1*	65796.36	5.7	Q07932	Pilosulin-1	*Myrmecia pilosula* (Jack jumper ant)
comp66861_c0_seq1*	15029.07	9.00E−06	Q7LZF5	Thrombin-like enzyme catroxobin-1	*Crotalus atrox* (Western diamond-back rattlesnake)
comp63353_c0_seq1*	13650.81	2.2	P0DMA1	Conotoxin pc3a	*Conus pictus* (Cone snail)
comp20403_c0_seq1	5282.15	5.00E−24	Q9YGJ9	Snake venom serine protease Haly-2	*Gloydius brevicaudus* (Korean slamosa snake)
comp62074_c0_seq3	2558.95	7.3	P0C176	Peptide TsPep3	*Tityus serrulatus* (Brazilian scorpion)
comp52195_c0_seq1	1794.84	0.67	B1P1H1	Kappa-theraphotoxin-Cg1d	*Chilobrachys guangxiensis* (Chinese earth tiger tarantula)
comp53334_c0_seq1*	**1783.89**	**4.4**	**P0C2B0**	**Conotoxin ViVA**	***Conus virgo* (Virgin cone)**
comp35599_c0_seq1	**1710.94**	**1.4**	**Q95WD1**	**Toxin CsE8**	*Centruroides sculpturatus* (Bark scorpion)
comp59348_c0_seq1	1703.65	4.00E−06	P0DJG3	Thrombin-like enzyme TLBan	*Bothrocophias andianus (*Andean lancehead)
comp54362_c0_seq1	**1523.38**	**1.00E−19**	**G3LU44**	**Translationally-controlled tumor protein homolog**	*Loxosceles intermedia* (Brown spider)
Transcript	**TP FKPM**	***E*-value**	**ID**	**Protein names**	**Organism**
comp68091_c0_seq1*	8457.37	0.086	B6DD38	U14-lycotoxin-Ls1a	*Lycosa singoriensis* (Wolf spider) (*Aranea singoriensis*)
comp76287_c0_seq3*	4081.53	7.00E−04	A7X4K7	Waprin-Phi2	*Philodryas olfersii* (Green snake)
comp75135_c0_seq1*	2777.31	4.2	Q9BJV8	Omega-hexatoxin-Asp2a	*Atrax* sp. (strain Illawarra) (Funnel-web spider)
comp53334_c0_seq1*	**2667.8**	**4.4**	**P0C2B0**	**Conotoxin ViVA**	***Conus virgo* (Virgin cone)**
comp35599_c0_seq1	**2478.75**	**1.4**	**Q95WD1**	**Toxin CsE8**	***Centruroides sculpturatus* (Bark scorpion)**
comp54362_c0_seq1	**2247.73**	**1.00E−19**	**G3LU44**	**Translationally-controlled tumor protein homolog**	***Loxosceles intermedia* (Brown spider)**
comp35571_c0_seq1	2145.5	1.7	G1AS77	Conotoxin Vc6.11	*Conus victoriae* (Queen Victoria cone)
comp77096_c0_seq1	2004.16	0.42	Q5Y4V3	U3-agatoxin-Ao1f	*Agelena orientalis* (Spider)
comp78185_c0_seq1	1775.11	7	P86990	Non-toxic venom protein	*Rhopalurus junceus* (Caribbean blue scorpion)
comp57678_c0_seq1	1691.18	1.9	B3FIU2	U12-theraphotoxin-Hs1a	*Haplopelma schmidti* (Chinese bird spider)
SignalP Top BLAST hits					
Transcript	**GC FKPM**	***E*-value**	**ID**	**Protein names**	**Organism**
comp63246_c0_seq1*	65796.36	0.37	Q0TXH0	Eukaryotic translation initiation factor 3 subunit K	*Phaeosphaeria nodorum* (Glume blotch fungus)
comp78135_c0_seq1	56621.03	3.84E−11	Q60648	Ganglioside GM2 activator	*Mus musculus* (Mouse)
comp20389_c0_seq1	28885.47	1.52E−53	P40313	Chymotrypsin-like protease CTRL-1	*Homo sapiens* (Human)
comp76457_c0_seq1	24676.96	8.5	Q5FCW3	Putative elongation factor Tu-like protein	*Ehrlichia ruminantium* (strain Welgevonden)
comp61419_c0_seq1	19420.18	1.86E−84	P48052	Carboxypeptidase A2	*Homo sapiens* (Human)
comp53328_c1_seq1	16975.74	—	—	—	—
comp53348_c0_seq1	16780.85	1.3	Q7XVM8	Transport inhibitor response 1-like protein Os04g0395600	*Oryza sativa* subsp. *japonica* (Rice)

(continued)

Table 2 Continued

			ToxProt Top BLAST hits		
Transcript	**GC FKPM**	***E*-value**	**ID**	**Protein names**	**Organism**
comp66861_c0_seq1*	15029.07	7.67E−51	P08419	Chymotrypsin-like elastase family member 2A	*Sus scrofa* (Pig)
comp62035_c0_seq1	14625.55	2.28E−46	B8V7S0	CUB and peptidase domain-containing protein 1	*Acropora millepora* (Staghorn coral)
comp63353_c0_seq1*	13650.81	8.29E−57	P04813	Chymotrypsinogen 2	*Canis lupus familiaris* (Dog)
Transcript	**TP FKPM**	***E*-value**	**ID**	**Protein names**	**Organism**
comp68091_c0_seq1*	8457.37	2.4E−58	Q6P4Z2	Collagen alpha-1	*Xenopus tropicalis* (Western clawed frog)
comp35596_c0_seq1	8436.25	1.22E−62	P02466	Collagen alpha-2	*Rattus norvegicus* (Rat)
comp67666_c0_seq1	7038.22	3.3	Q9C9L5	Wall-associated receptor kinase-like 9	*Arabidopsis thaliana* (Mouse-ear cress)
comp76287_c0_seq3*	4081.53	2.44E−51	B8V7R6	Collagen alpha chain	*Acropora millepora* (Staghorn coral)
comp78195_c0_seq1	3708.28	—	—	—	—
comp63341_c0_seq1	3257.39	7.08E−128	Q26636	Cathepsin L	*Sarcophaga peregrina* (Flesh fly)
comp75135_c0_seq1*	2777.31	1.1E−62	Q9U943	Apolipophorins [Cleaved into: Apolipophorin-2]	*Locusta migratoria* (Migratory locust)
comp53334_c0_seq1*	2667.8	0	P63018	Heat shock cognate 71 kDa protein	*Rattus norvegicus* (Rat)
comp63348_c0_seq1	2591.46	1.37E−22	Q9VQ62	Protein NPC2 homolog	*Drosophila melanogaster* (Fruit fly)
comp20388_c0_seq1	2388.4	4.17E−91	Q7ZWJ4	60S ribosomal protein L18a	*Danio rerio* (Zebrafish)

Notes: Duplicate hits within each search are noted in bold. * indicates transcript identified using both approaches.

binding activity (of small molecules and ions) were the most abundant (Fig. 5); these functional groups were consistently most highly representative of the gastric cirri. Conversely, GO groups assigned to tentacle/pedalium were much less abundant, with the most highly expressed transcripts in the BP and MF domains associated with translation and structural molecules, respectively (Fig. 5).

Within the gastric cirri, many of the more highly expressed GO groups identified in our analysis were linked to multiple transcripts. Based on UniProt BLAST hits, dozens of transcripts (and in some instances more than one hundred transcripts) were linked to BP domains such as proteolysis [GO:0006508], digestion [GO:0007586], transcription and DNA-templated [GO:0006351], and to MF domains such as serine-type endopeptidase activity [GO:0004252], zinc-ion binding [GO:0008270], and metallopeptidase activity [GO:0004222]. This suggests that although collectively these functional groups might play key roles in the gastric cirri, there were no single candidate transcripts exhibiting a primary functional role in the gastric cirri. However, some GO groups were specific to a select few transcripts, despite being expressed at higher levels. For example, motor activity [GO:0003774] in the MF domain was highly abundant, although exclusively linked to four BLAST hits matching myosin genes. Additionally, establishment of skin barrier [GO:0061436] was associated with two transcripts identified as chymotrypsin-like proteins, which have been identified as venom components in other cnidarians (Rottini et al. 1995; Gusmani et al. 1997).

Within the tentacle/pedalium, transcripts associated with the BP domain were expressed at much lower levels than those within the gastric cirri, with many transcripts corresponding to the broad GO term cellular response to stimulus [GO:0051716]. In the MF domain, however, there were over one hundred transcripts associated with metal ion binding [GO:0046872] and ATP binding [GO:0005524], although these GO groups collectively corresponded to transcripts expressed at much lower levels in the tentacles when compared with the GO outputs of the gastric cirri (Fig. 4). Finally, there were over a dozen transcripts belonging to the extracellular matrix structural constituent [GO:0005201], sharing high sequence similarity to collagens, fibrillins, and other structural proteins. Collectively these GO associations illustrate that the gene products involved in digestion are numerous, with no single GO group

existing in great abundance across transcripts exhibiting a typical digestive or venom functional role. Furthermore, the abundant GO groups within the tentacles do not resemble any of the large gene families commonly recruited into venom assemblages (Fry et al. 2009). A full list of GO groups and associated transcripts is provided in Supplementary File S3.

Additional toxin candidates

Previous transcriptome profiling of the tentacle/pedalium of *A. alata* (Lewis Ames et al. 2016) did not conclusively identify an abundance of likely bioactive protein candidates that might be responsible for inducing *A. alata* envenomation symptoms (see Chung et al. 2001; Figueroa Rosa 2015). Among the ~32K transcripts comprising the *A. alata* transcriptome, we identified 1787 toxin-like transcripts that shared sequence similarity to known toxin genes, but that had not been identified previously in the *A. alata* transcriptome. Of these, 578 transcripts contained a signaling peptide region. Similarly to the initial gene expression analyses we conducted, our findings here also show that the more abundant candidate toxins are found within the gastric cirri rather than the tentacle/pedalium (Table 2). Using the program SignalP we identified 3517 transcripts containing a signaling region, many of which did not resemble known toxin genes. However, these results showed that transcripts containing a signaling region were also consistently more abundant in the gastric cirri than in the tentacle (Table 1). Ultimately, we found that the tentacle/pedalium did not exhibit comparatively high expression levels of any candidate toxins that might be correlated with envenomation symptoms. Unexpectedly, when screening the tentacle/pedalium transcriptome against the ToxProt data set, the four most highly expressed toxin-like transcripts had higher sequence similarity to proteins that are non-toxic from the SignalP analysis (Table 2). This may be indicative of structural gene products that share similar protein motifs with venom from other taxa rather than the identified transcripts being actual toxins. Despite using several approaches to analyze these candidates herein, all structural genes with known roles in nematogenesis were consistently and exclusively expressed at high levels in the tentacle/pedalium, while toxin-like transcripts were consistently expressed at proportionately higher levels in the gastric cirri (Figs. 4 and 5; Table 2). Our findings corroborate the report of multiple homologs of the CaTX toxin family being expressed in a tissue-specific manner in the tentacle/pedalium and gastric cirri of *A. alata*, and with fewer homologs identified in the tentacle/pedalium (Lewis Ames et al. 2016). Expression of CaTX, a pore-forming toxin, in the tentacle/pedalium, even in small amounts, suggests some production does occur in the tentacle/pedalium of *A. alata*, as has also been reported in other jellyfish species in which only the tentacle or extracted nematocyst venom has been analyzed (Nagai et al. 2000a, 2000b; Brinkman and Burnell 2009; Li et al. 2014; Brinkman et al. 2015; Jouiaei et al. 2015a; Ponce et al. 2016). However, given the comparatively low abundance of genes for known bioactive proteins expressed in the tentacle/pedalium (compared with the gastric cirri), it is possible that most candidate toxin proteins deployed by *A. alata* tentacles during envenomation are synthesized elsewhere (i.e., the gastric cirri) and transported to the tentacle as pre-packaged proteins. Alternatively, tentacle venom components might be expressed in the tentacle/pedalium at levels low enough to evade detection in this study, or simply remain to be characterized in this cubozoan species.

Conclusion

In this study, our combined molecular and morphological analyses revealed that transcripts encoding putative toxins and toxic-like enzymes are almost exclusively expressed in the gastric cirri of the box jellyfish *Alatina alata*. Therefore, expression of venom-implicated genes does not primarily occur in the tentacle where venom deployment typically occurs in cubozoans. Given our observations of putative gland cells associated with the gastric cirri, we speculate that granules secreted by the gastric cirri of *A. alata* contain a concoction of dual-function digestive enzymes and venom components, as is also reflected in the results of the transcriptome profiling of the gastric cirri in this study. Our findings, which are atypical of cnidarians, suggest that the presence of an assemblage of putative gland cells in the stomach predates the emergence of gastric cirri. Furthermore, we propose that protein components corresponding to toxins and toxic-like enzymes, secreted by putative glands cells, may be recruited for novel venom-related roles in the tentacles and nematocyst warts where nematocysts are in highest abundance. In the future, expanding on this preliminary combined morphological and transcriptomic approach to include other cubozoans, in particular those lacking gastric cirri, may elucidate the potential role of gland cells in secretion of venom and digestion proteins.

Supplementary data

Supplementary data available at *ICB* online.

Acknowledgments

We thank Scott Tuason and Ron N. Larson for providing consent to use their photos, Austin Lin and Allen G. Collins for help with photos and videos, Bud Gillan for facilitating connections, and A. Lynn Mac and A. J. Umibito for assistance with data analysis. Data were analyzed on the Smithsonian High Performance Computing Cluster Hydra and the Ohio Biodiversity Conservation Partnership (OBCP) cluster. Finally, we express our gratitude to two external reviewers whose comments and suggested revisions helped improve the manuscript, and to the Managing Editor Suzanne Miller.

Funding Statement

Funding for CLA to complete this study was provided through an Ann G. Wylie Dissertation Fellowship from the Graduate School of the University of Maryland, and for photography through support from Allen G. Collins who acknowledges the Mary and Robert Pew Public Education Fund. An earlier version of this work was presented at the SICB venom symposium thanks to support from Marymegan Daly who acknowledges US National Science Foundation DEB-1257796.

References

Acevedo MJ, Fuentes VL, Olariaga A, Canepa A, Belmar MB, Bordehore C, Calbet A. 2013. Maintenance, feeding and growth of *Carybdea marsupialis* (Cnidaria: Cubozoa) in the laboratory. J Exp Mar Bio Ecol 439:84–91.

Anderluh G, Podlesek Z, Maček P. 2000. A common motif in proparts of Cnidarian toxins and nematocyst collagens and its putative role. Biochim Biophys Acta 1476:372–6.

Arneson AC, Cutress CE. 1976. Life history of *Carybdea alata* Reynaud, 1830 (Cubomedusae). New York: Plenum Publishing Corporation. p. 227–36

Avila SG. 2009. Molecular characterization of *Carukia barnesi* and *Malo kingi*, cnidaria; Cubozoa; Carybdeidae [PhD thesis]. James Cook University.

Balasubramanian PG, Beckmann A, Warnken U, Schnölzer M, Schüler A, Bornberg-Bauer E, Holstein TW, Ozbek S. 2012. Proteome of *Hydra* nematocyst. J Biol Chem 287:9672–81.

Barnes JH. 1966. Studies on three venomous Cubomedusae. London and New York: Academic Press.

Basulto A, Perez V, Noa Y, Varela C, Otero AJ, Pico MC. 2006. Immunohistochemical targeting of sea anemone cytolysins on tentacles, mesenteric filaments and isolated nematocysts of *Stichodactyla helianthus*. J Exp Zool A Comp Exp Biol 305A:253–8.

Beckmann A, Özbek S. 2012. The nematocyst: a molecular map of the cnidarian stinging organelle. Int J Dev Biol 56:577–82.

Bentlage B, Cartwright P, Yanagihara AA, Lewis C, Richards GS, Collins AG. 2010. Evolution of box jellyfish (Cnidaria: Cubozoa), a group of highly toxic invertebrates. Proc R Soc B Biol Sci 277:493–501.

Bentlage B, Lewis C. 2012. An illustrated key and synopsis of the families and genera of carybdeid box jellyfishes (Cnidaria: Cubozoa: Carybdeida), with emphasis on the "Irukandji family" (Carukiidae). J Nat Hist 46:2595–620.

Bottrall JL, Madaras F, Biven CD, Venning MG, Mirtschin PJ. 2010. Proteolytic activity of Elapid and Viperid snake venoms and its implication to digestion. J Venom Res 1:18–28.

Brinkman DL, Burnell JN. 2009. Biochemical and molecular characterisation of cubozoan protein toxins. Toxicon 54:1162–73.

Brinkman DL, Jia X, Potriquet J, Kumar D, Dash D, Kvaskoff D, Mulvenna J. 2015. Transcriptome and venom proteome of the box jellyfish *Chironex fleckeri*. BMC Genomics 16:407.

Calvete JJ, Sanz L, Angulo Y, Lomonte B, Gutiérrez JM. 2009. Venoms, venomics, antivenomics. FEBS Lett 583:1736–43.

Carrette T, Alderslade P, Seymour J. 2002. Nematocyst ratio and prey in two Australian cubomedusans, *Chironex fleckeri* and *Chiropsalmus* sp. Toxicon 40:1547–51.

Carrette T, Straehler-Pohl I, Seymour J. 2014. Early life history of *Alatina* cf. *moseri* populations from Australia and Hawaii with implications for taxonomy (Cubozoa: Carybdeida, Alatinidae). PLoS One 9:e84377.

Casewell NR, Wüster W, Vonk FJ, Harrison RA, Fry BG. 2012. Complex cocktails: the evolutionary novelty of venoms. Trends Ecol Evol 28:219–29.

Chera S, de Rosa R, Miljkovic-Licina M, Dobretz K, Ghila L, Kaloulis K, Galliot B. 2006. Silencing of the *Hydra* serine protease inhibitor Kazal1 gene mimics the human SPINK1 pancreatic phenotype. J Cell Sci 119:846–57.

Chiaverano LM, Holland BS, Crow GL, Blair L, Yanagihara AA. 2013. Long-term fluctuations in circalunar Beach aggregations of the box jellyfish *Alatina moseri* in Hawaii, with links to environmental variability. PLoS One 8:e77039.

Chung JJ, Ratnapala LA, Cooke IM, Yanagihara AA. 2001. Partial purification and characterization of a hemolysin (CAH1) from Hawaiian box jellyfish (*Carybdea alata*) venom. Toxicon 39:981–90.

Collins AG, Bentlage B, Gillan W, Marques AC. 2011. Naming the Bonaire banded box jelly, *Tamoya ohboya*, n. sp. (Cnidaria: Cubozoa: Carybdeida: Tamoyidae). Zootaxa 68:53–68.

Conant FS. 1897. Notes on the cubomedusae. Johns Hopkins University Circ 132:8–10.

Conant FS. 1898. The cubomedusae. By Franklin Story Conant. A memorial volume. Memoirs from the biological laboratory of the Johns Hopkins University, IV, 1. Baltimore: The Johns Hopkins Press.

David CN, Challoner D. 1974. Distribution of interstitial cells and differentiating nematocytes in nests in *Hydra attenuata*. Am Zool 14:537–42.

David CN, Ozbek S, Adamczyk P, Meier S, Pauly B, Chapman J, Hwang JS, Gojobori T, Holstein TW. 2008. Evolution of complex structures: minicollagens shape the cnidarian nematocyst. Trends Genet 24:431–8.

Di Camillo C, Bo M, Puce S, Bavestrello G. 2006. The cnidome of *Carybdea marsupialis* (Cnidaria: Cubomedusae) from the Adriatic Sea. J Mar Biol Assoc UK 86:705.

Fautin D, Mariscal R. 1991. Cnidaria: Anthozoa. In: Harrison FW, Westfall JA, editors. Microscopic anatomy of invertebrates, volume 2: Placozoa, Porifera, Cnidaria, and

Ctenophora. New York and other cities. Wiley- Liss, Inc. p. 267–358.
Felsenstein J. 2009. version 3.7a. Distributed by the author. Department of Genome Sciences, University of Washington, Seattle.
Figueroa Rosa BJ. 2015. Mucho ojo con las aguavivas. Primerahora.
Fry BG, Roelants K, Champagne DE, Scheib H, Tyndall JD, King GF, Nevalainen TJ, Norman JA, Lewis RJ, Norton RS, et al. 2009. The toxicogenomic multiverse: convergent recruitment of proteins into animal venoms. Annu Rev Genomics Hum Genet 10:483–511.
Gacesa R, Chung R, Dunn SR, Weston AJ, Jaimes-Becerra A, Marques AC, Morandini AC, Hranueli D, Starcevic A, Ward M, et al. 2015. Gene duplications are extensive and contribute significantly to the toxic proteome of nematocysts isolated from *Acropora digitifera* (Cnidaria: Anthozoa: Scleractinia). BMC Genomics 16:774.
Gershwin L-A. 2006. Nematocysts of the Cubozoa. Zootaxa 57:1–57.
Gershwin L-A. 2005. *Carybdea alata* auct. and *Manokia stiasnyi*, reclassification to a new family with description of a new genus and two new species. Mem Queensl Museum 51:501–23.
Gershwin L-A, De Nardi M, Winkel KD, Fenner PJ. 2010. Marine stingers: review of an under-recognized global coastal management issue. Coast Manag 38:22–41.
Gnerre S, Maccallum I, Przybylski D, Ribeiro FJ, Burton JN, Walker BJ, Sharpe T, Hall G, Shea TP, Sykes S, et al. 2011. High-quality draft assemblies of mammalian genomes from massively parallel sequence data. Proc Natl Acad Sci USA 108:1513–8.
Grabherr MG, Haas BJ, Yassour M, Levin JZ, Thompson DA, Amit I, Adiconis X, Fan L, Raychowdhury R, Zeng Q, et al. 2011. Full-length transcriptome assembly from RNA-Seq data without a reference genome. Nat Biotechnol 29:644–52.
Gusmani L, Avian M, Galil B, Patriarca P, Rottini G. 1997. Biologically active polypeptides in the venom of the jellyfish *Rhopilema nomadica.* Toxicon 35:637–48.
Haas BJ, Papanicolaou A, Yassour M, Grabherr M, Blood PD, Bowden J, Couger MB, Eccles D, Li B, Lieber M, et al. 2013. De novo transcript sequence reconstruction from RNA-seq using the Trinity platform for reference generation and analysis. Nat Protoc 8:1494–512.
Hamner W, Jones M, Hamner P. 1995. Swimming, feeding, circulation and vision in the Australian box jellyfish, *Chironex fleckeri* (Cnidaria: Cubozoa). Mar Freshw Res 46:985–90.
Hessinger DA, Lenhoff HM. 1988. The biology of nematocysts. Academic Press Inc.
Ishida J. 1936. Note on the digestion of *Charybdea rastonii.* Annot Zool Japan15:449–52.
Jouiaei M, Casewell NR, Yanagihara AA, Nouwens A, Cribb BW, Whitehead D, Jackson TN, Ali SA, Wagstaff SC, Koludarov I, et al. 2015a. Firing the sting: chemically induced discharge of cnidae reveals novel proteins and peptides from box jellyfish (*Chironex fleckeri*) venom. Toxins (Basel) 7:936–50.
Jouiaei M, Yanagihara AA, Madio B, Nevalainen TJ, Alewood PF, Fry BG. 2015b. Ancient venom systems: a review on Cnidaria toxins. Toxins (Basel) 7:2251–71.
Júnior MN, Haddad MA. 2008. The diet of cubomedusae (cnidaria, cubozoa) in southern Brazil. Brazilian Journal of Oceanography 56:157–64.
Junqueira-de-Azevedo ILM, Bastos CMV, Ho PL, Luna MS, Yamanouye N, Casewell NR. 2015. Venom-related transcripts from *Bothrops jararaca* tissues provide novel molecular insights into the production and evolution of snake venom. Mol Biol Evol 32:754–66.
Katoh K, Standley DM. 2013. MAFFT multiple sequence alignment software version 7: improvements in performance and usability. Mol Biol Evol 30:772–80.
Kearse M, Moir R, Wilson A, Stones-Havas S, Cheung M, Sturrock S, Buxton S, Cooper A, Markowitz S, Duran C, et al. 2012. Geneious Basic: an integrated and extendable desktop software platform for the organization and analysis of sequence data. Bioinformatics 28:1647–9.
Krueger F. 2012. Trim Galore! (http://www.bioinformatics.babraham.ac.uk/projects/trim galore/).
Langmead B, Trapnell C, Pop M, Salzberg SL. 2009. Ultrafast and memory-efficient alignment of short DNA sequences to the human genome. Genome Biol 10:R25.
Larson RJ. 1976. Cubomedusae: feeding functional morphology, behavior and phylogenetic position. In: Mackie GO, editor. Coelenterate ecology and behavior. Boston (MA): Springer. p. 237–45.
Lawley JW, Lewis Ames C, Bentlage B, Yanagihara A, Goodwill R, Kayal E, Hurwitz K, Collins AG. 2016. The box jellyfish *Alatina alata* has a circumtropical distribution. Biol Bull. 231(2).
Lewis Ames C, Ryan JF, Bely AE, Cartwright P, Collins AG. 2016. A new transcriptome and transcriptome profiling of adult and larval tissue in the box jellyfish *Alatina alata*: an emerging model for studying venom, vision and sex. BMC Genomics. 17:650.
Lewis C, Bentlage B, Yanagihara AA, Gillan W, Blerk JV, Keil DP, Bely AE, Collins AG. 2013. Redescription of *Alatina alata* (Reynaud, 1830) (Cnidaria: Cubozoa) from Bonaire, Dutch Caribbean. Zootaxa 3737:473–87.
Li B, Dewey CN. 2011. RSEM: accurate transcript quantification from RNA-Seq data with or without a reference genome. BMC Bioinformatics 12:323.
Li R, Yu H, Xue W, Yue Y, Liu S, Xing R, Li P. 2014. Jellyfish venomics and venom gland transcriptomics analysis of *Stomolophus meleagris* to reveal the toxins associated with sting. J Proteomics 106:17–29.
Mackessy SP, Williams K, Ashton KG. 2003. Ontogenetic variation in venom composition and diet of *Crotalus oreganus concolor*: a case of venom paedomorphsis? Copeia 2003:769–82.
Macrander J, Broe M, Daly M. 2016. Tissue-specific venom composition and differential gene expression in sea anemones. Genome Biol Evol published online (doi: 10.1093/gbe/evw155).
Macrander J, Broe M, Daly M. 2015. Multi-copy venom genes hidden in de novo transcriptome assemblies, a cautionary tale with the snakelocks sea anemone *Anemonia sulcata* (Pennant, 1977). Toxicon 108:184–8.
Mali B, Möhrlen F, Frohme M, Frank U. 2004. A putative double role of a chitinase in a cnidarian: pattern formation and immunity. Dev Comp Immunol 28:973–81.

McClounan S, Seymour J. 2012. Venom and cnidome ontogeny of the cubomedusae *Chironex fleckeri*. Toxicon 60:1335–41.

Moran Y, Genikhovich G, Gordon D, Wienkoop S, Zenkert C, Ozbek S, Technau U, Gurevitz M. 2012. Neurotoxin localization to ectodermal gland cells uncovers an alternative mechanism of venom delivery in sea anemones. Proc R Soc B Biol Sci 279:1351–8.

Moran Y, Praher D, Schlesinger A, Ayalon A, Tal Y, Technau U. 2013. Analysis of soluble protein contents from the nematocysts of a model sea anemone sheds light on venom evolution. Mar Biotechnol 15:329–39.

Nagai H, Takuwa K, Nakao M, Ito E, Miyake M, Noda M, Nakajima T. 2000a. Novel proteinaceous toxins from the box jellyfish (sea wasp) *Carybdea rastoni*. Biochem Biophys Res Commun 275:582–8.

Nagai H, Takuwa K, Nakao M, Sakamoto B, Crow GL, Nakajima T. 2000b. Isolation and characterization of a novel protein toxin from the Hawaiian Box Jellyfish (sea wasp) *Carybdea alata*. Biochem Biophys Res Commun 275:589–94.

Nevalainen TJ, Peuravuori HJ, Quinn RJ, Llewellyn LE, Benzie JA, Fenner PJ, Winkel KD. 2004. Phospholipase A2 in Cnidaria. Comp Biochem Physiol B Biochem Mol Biol 139:731–5.

Ozbek S. 2011. The cnidarian nematocyst: a miniature extracellular matrix within a secretory vesicle. Protoplasma 248:635–40.

Özbek S, Balasubramanian PG, Holstein TW. 2009. Cnidocyst structure and the biomechanics of discharge. Toxicon 54:1038–45.

Pan TL, Gröger H, Schmid V, Spring J. 1998. A toxin homology domain in an astacin-like metalloproteinase of the jellyfish *Podocoryne carnea* with a dual role in digestion and development. Dev Genes Evol 208:259–66.

Petersen TN, Brunak S, von Heijne G, Nielsen H. 2011. SignalP 4.0: discriminating signal peptides from transmembrane regions. Nat Methods 8:785–6.

Ponce D, Brinkman DL, Luna-Ramirez K, Wright CE, Dorantes-Aranda JJ. 2015. Comparative study of the toxic effects of *Chrysaora quinquecirrha* (Cnidaria: Scyphozoa) and *Chironex fleckeri* (Cnidaria: Cubozoa) venoms using cell-based assays. Toxicon 106:57–67.

Ponce D, Brinkman DL, Potriquet J, Mulvenna J. 2016. Tentacle transcriptome and venom proteome of the Pacific Sea Nettle, *Chrysaora fuscescens* (Cnidaria: Scyphozoa). Toxins (Basel) 8:102.

Price MN, Dehal PS, Arkin AP. 2010. FastTree 2 approximately maximum-likelihood trees for large alignments. PLoS One 5:e9490.

Rachamim T, Morgenstern D, Aharonovich D, Brekhman V, Lotan T, Sher D. 2014. The dynamically evolving nematocyst content of an anthozoan, a scyphozoan, and a hydrozoan. Mol Biol Evol 32:740–53.

Robinson MD, McCarthy DJ, Smyth GK. 2010. EdgeR: a bioconductor package for differential expression analysis of digital gene expression data. Bioinformatics 26:139–40.

Rottini G, Gusmani IL, Parovel IE, Avian M, Patriarca P. 1995. Purification and properties of a cytolytic toxin in venom of the jellyfish *Carybdea marsupialis*. Toxicon 33:315–26.

Slautterback DB, Fawcett DW. 1959. The development of the cnidoblasts of *Hydra*. An electron microscope study of cell differentiation. J Biophys Biochem Cytol 5:441–52.

Southcott RV. 1967. Revision of some carybdeidae (Scyphozoa: Cubomedusae), including a description of the jellyfish responsible for the ''Irukandji syndrome.'' Aust J Zool 15:651–71.

Stewart SE. 1996. Field behavior of *Tripedalia cystophora* (class cubozoa). Mar Freshw Behav Physiol 27:175–88.

Supek F, Bosnjak M, Skunca N, Smuc T. 2011. Revigo summarizes and visualizes long lists of gene ontology terms. PLoS One published online (doi:10.1371/journal.pone.0021800).

Zenkert C, Takahashi T, Diesner M-O, Özbek S. 2011. Morphological and molecular analysis of the *Nematostella vectensis* cnidom. PLoS One 6:e22725.